

NATIONAL AIR INTELLIGENCE CENTER



REAL TIME CORRELATING OPERATION ON DIFFUSE OBJECTS

by

Wang Tianji, Yang Shining,
Li Yao Tang and Zhang Shi Chao



DTIC QUALITY INSPECTED B

Approved for public release;
Distribution unlimited.

19950407 124

GRAPHICS DISCLAIMER

All figures, graphics, tables, equations, etc. merged into this translation were extracted from the best quality copy available.

TABLE OF CONTENTS

GRAPHICS DISCLAIMER	i
Table of Contents	ii
Real Time Correlating Operation on Diffuse Objects	1

Wang Tianji, Yang Shining, Li Yao Tang and Zhang Shi Chao¹

I. Introduction

Real time correlating operations on diffuse objects are an expansion and outgrowth on 2-D transparent objects. A real time optical correlator with two transparent pieces is made using photorefractive crystal $\text{Bi}_{12}\text{SiO}_{20}$ (BSO) and noncrystal membrane As_2S_3 as recording media [1-3]. Due to the absence of wave filter that is associated with the typical real time optical correlator, this enables the two transparent pieces to have real time correlation and have potential applications in feature recognition. However, test object and reference object have to be in transparent state. In reality, most objects that need to be recognized tend to be diffuse objects, or they have to rely on natural light (incoherent light) for lightening. The realization of real time correlation on two diffuse objects or incoherent light images remains to be fulfilled.

Duthie et al made compact real time optical correlators from liquid crystal image convertor [4]. Liu [5] and Mcewan [6] et al proposed modifying the inexpensive liquid crystal TV's that are sold on the market into a convenient and cheap spatial optical modulator. With this in mind, we modified a liquid crystal TV into an incoherent to coherent convertor. Using it in conjunction with BSO crystals constitutes a real time correlator on diffuse objects.

* Numbers in margins indicate foreign pagination.
Commas in numbers indicate decimals.

¹ Canton Institute of Electronic Technology, Academia Sinica.

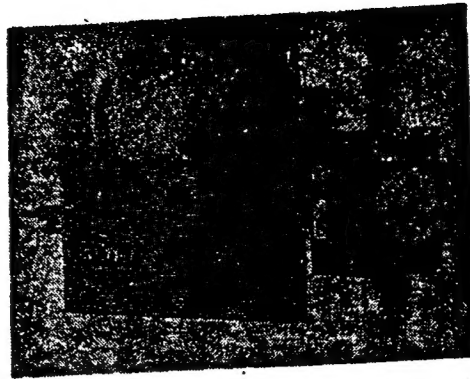


Fig. 1 Photograph of the LCTV spatial light modulator

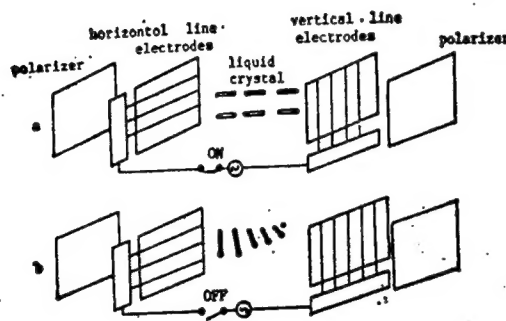


Fig. 2 Operating principle of the LCTV spatial light modulator

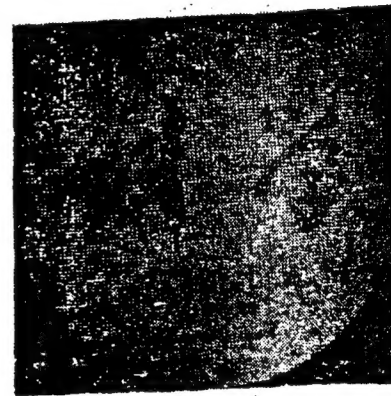


Fig. 3 Photograph of the coherent reverse image via LCTV spatial light modulator

II. Liquid Crystal TV Spatial Optical Modulator

Liquid crystal TV can be made into a spatial optical modulator. Size of black and white liquid crystal TV CITIZEN 08TA-OH is $71 \times 53 \text{ mm}^2$ with 160×130 pixels. Fig.1 is the modified spatial optical modulator. By removing all glasses and membranous polarizer and modifying the electric circuit so that outside TV signals can be received, and by adding advanced polarizer, the output signals of the video camera can be displayed on liquid crystal TV.

/1029

Fig.2 is the schematic diagram of the liquid crystal TV spatial optical modulator. There are two electrodes

(horizontal and vertical) between the interface of liquid crystal and two glass plates. Outside the two plates, there are two polarizers in parallel. In the absence of electrical field between the two transparent electrodes, columns of liquid crystal molecules rotate 90° due to the twist of polarizing surface, no light will be able to pass through the second polarizer. In the presence of electrical field, liquid crystal molecules realign in the direction of electrical field, light will be able to pass through the second polarizer. The image recorded by video camera will be converted to electrical signals and exported to the liquid crystal TV. By shining beams of coherent light to the screen of the liquid crystal TV, a coherent image will be formed. Thus, a conversion of incoherent image to coherent one is completed by the liquid crystal TV(LCTV) spatial optical modulator. Fig.3 is a photo of a converted coherent image by passing a diffuse object through LCTV spatial light modulator.

III. Diffuse object's Real Time Correlating Operation System

Using LCTV spatial optical modulator, an incoherent image on diffuse objects can be converted to coherent image and be exported to real time correlator made of BSO crystal for further operation.

Fig.4 depicts the scheme of this system. Diffuse object T is recorded by video camera and the image is transmitted to LCTV after shined by incoherent light. Laser λ_1 shines on the LCTV screen and reference object R, the resulting hologram on R and T is recorded on BSO crystal. Using $\lambda_2=633$ nm He-Ne laser, a phased hologram can be obtained. After Fourier transformation, an expression for the diffraction observed behind the focal plane of lens L_2 is

$$|T(x_s, y_s)|^2 = \delta(x_s, y_s) + \beta^2 \left| A \otimes A^* + B \otimes B^* + A \otimes B^* \otimes \delta\left(x_s - 2\xi \frac{\lambda_2 f_2}{\lambda_1 f_1}, y_s\right) + A^* \otimes B \otimes \delta\left(x_s + 2\xi \frac{\lambda_2 f_2}{\lambda_1 f_1}, y_s\right) \right|^2.$$

The correlating peaks for R and T are the two shining spots each with a distance $\left| 2\xi \frac{\lambda_2 f_2}{\lambda_1 f_1} \right|$ away from the central point.

The size of BSO crystal is $10 \times 10 \times 2 \text{ mm}^2$, the voltage exerted on the BSO crystal by GE-2 BSO crystal high power source is 6 kV/cm. A transverse high voltage is in the direction of crystal (110), light beam projects from (110) records hologram.

/1030

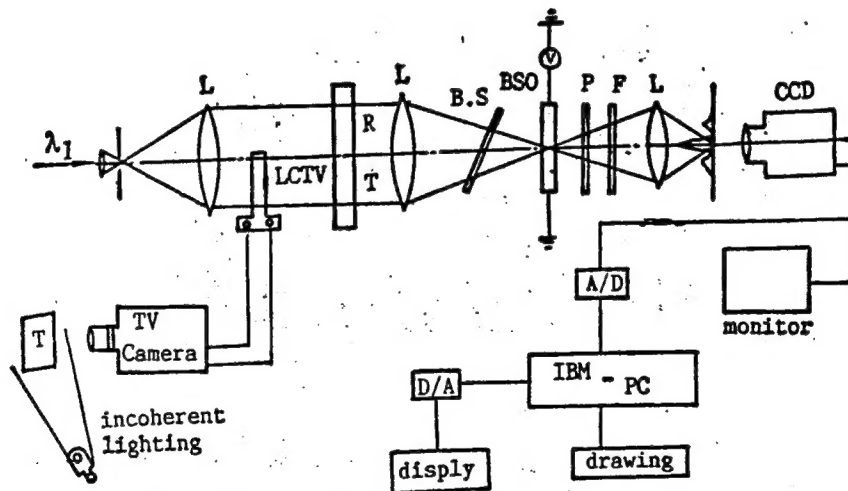


Fig. 4 Experimental arrangement for real-time cross correlating operation on diffuse object

On the correlating output plane, a CCD video camera(2048) scans the correlating peaks and records. The recorded signals are converted by A/D and entered into IBM PC for processing and analysis, the correlating peaks will be drawn by an automatic chart recorder.

IV. Results and Discussion

Fig.5 is the preliminary photo of test object and reference object and the photo of their correlation peak. In the experiment, we used the same English word "optics" as both reference and test object. Relative value of the correlating peaks is measured. As the structure of the test object changes, the intensity of the correlation peaks decreases to certain extent. Table 1 is the relative value of correlation peak measured when certain letters in word "optics" are changed. Fig.6 is a 2-D scanning of a correlation peak of two identical words.

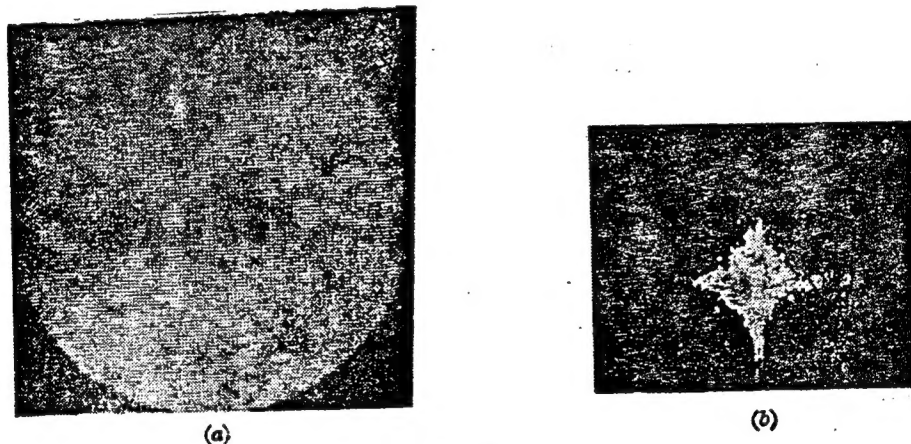


Fig. 5
(a) test object; (b) cross correlation peak

Use of LCTV spatial optical modulator as an incoherent image to coherent image convertor is both convenient and economical. By combining it with a photorefractive crystal BSO based real time correlator, a real time correlating operation on a diffuse object can be carried out. This is one of the features of this study. More over, combination of the real time correlator with the analysis of the correlating peaks is a big step forward in correlation recognition study.

Table 1 Relative value of correlation peak when the test object changed

reference object	Optics	Optics	Optics	Optics	Optics	Optics
test object	Optics	t	ti	tics	ptics	Optics
average value of measzrment	1.391	1.126	1.220	1.274	1.306	1.326

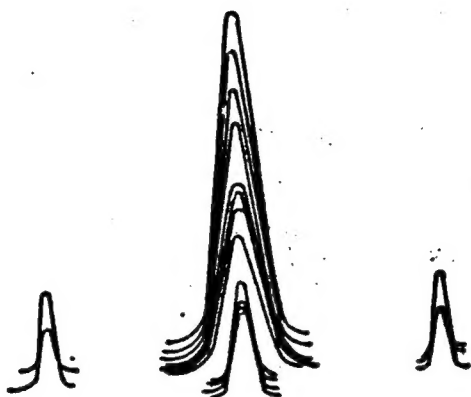


Fig. 6 Relative value of 2-D scanning correlation peak

During the test of the correlation recognition, if test object and reference object both locate on the X axis on the input plane, their correlation peak will show up on the X axis of the output plane. They are symmetric in relation to Y axis, and have coordinates $2\xi \frac{\lambda_2 f_2}{\lambda_1 f_1}$ and $2\xi \frac{\lambda_2 f_2}{\lambda_1 f_1}$ respectively. When the recording and displaying wavelength is constant, the distance between correlating peak and the central point is $\left| 2\xi \frac{\lambda_2 f_2}{\lambda_1 f_1} \right|$, which is dependent on the distance between the central point and the reference ξ and test object, and the focal length of lens L_1 and L_2 . If the

value of ξ changes, we must adjust the angle between the recording light beam λ_1 and displaying light beam λ_2 , causing θ_n , $\sin \theta_n = \frac{\lambda_2 \xi}{\lambda_1 f_1}$. As it is shown by Table 1, when the test and reference object are identical, the relative value of correlation peaks reaches a maximum. As they further diverge from each other, the relative value gradually decreases.

The scope of this study does not include the cases in which test objects experiences abrupt changes. The correlation operation on test objects whose size, direction, coordinates (rotation) vary, is an aim of another study elsewhere.

Acknowledgement: Fan Shao Wu and Wen Huan Ruong also contributed to this study.

REFERENCES

- [1] 王天及;《光学学报》, 1983, 3, No. 9 (Dec), 828~831.
- [2] T. J. Wang; "Conference of ICO-13", (Sappor '84, 1984), 166.
- [3] T. J. Wang; "Image Science '85", (Otanimi, Finland, 1985).
- [4] J. D. Duthine, J. Upatnieks; *Opt. Eng.*, 1984, 23, No. 1 (Jan), 7~11.
- [5] H. K. Liu; *Opt. Lett.*, 1985, 10, No. 12 (Dec), 635~637.
- [6] J. A. Mcswan, et al.; *J. Opt. Soc. Am.*; 1985, A2, No. 1, (Jan), 3~11.
- [7] C. Michael et al.; *Opt. Lett.*, 1987, 12, No. 8 (Aug), 549~551.

DISTRIBUTION LIST

DISTRIBUTION DIRECT TO RECIPIENT

<u>ORGANIZATION</u>	<u>MICROFICHE</u>
B085 DIA/RIS-2FI	1
C509 BALLOC509 BALLISTIC RES LAB	1
C510 R&T LABS/AVEADCOM	1
C513 ARRADCOM	1
C535 AVRADCOM/TSARCOM	1
C539 TRASANA	1
Q592 FSTC	4
Q619 MSIC REDSTONE	1
Q008 NTIC	1
Q043 AFMIC-IS	1
E051 HQ USAF/INET	1
E404 AEDC/DOF	1
E408 AFWL	1
E410 AFDTC/IN	1
E429 SD/IND	1
P005 DOE/ISA/DDI	1
P050 CIA/OCR/ADD/SD	2
1051 AFIT/LDE	1
P090 NSA/CDB	1
2206 FSL	1

Microfiche Nbr: FTD95C000091
NAIC-ID(RS)T-0373-94